JOURNAL OF CATALYSIS, 99, 400–414 (1986)

Nature and Mechanism of Formation of Vanadyl Pyrophosphate: Active Phase in *n*-Butane Selective Oxidation

GUIDO BUSCA,* FABRIZIO CAVANI,† GABRIELE CENTI,† AND FERRUCCIO TRIFIRÒ†,[1]

Istituto Chimico, Facoltà Ingegneria, Viale Risorgimento 2; and †Istituto Tecnologie Chimiche Speciali, Facoltà Chimica Industriale, Viale Risorgimento 4, 40136 Bologna, Italy

Received March 4, 1985; revised July 22, 1985

The preparation of vanadium–phosphorus catalysts from V_2O_5/H_3PO_4/benzyl- and isobutyl alcohols leads to the formation of $VOHPO_4 \cdot \frac{1}{2}H_2O$ with the organic alcohols trapped between the layers of the phosphate structure, which provoke disorder in the plane of layer stacking. During the successive calcination, a pseudomorphic $(VO)_2P_2O_7$ forms with corresponding disorder in the plane of layer stacking. Disorder in this plane influences: (i) the catalytic activity in *n*-butane selective oxidation, and (ii) the redox properties of the catalyst, both modifying the rate of vanadium(IV) oxidation to V(V) and the reducibility of the catalyst in a flow of 1% *n*-butane/air. It is suggested that during calcination the alcohol induces the formation of local structural deformations which are responsible for the increase of activity in *n*-butane, but not in 1-butene, selective oxidation of the catalysts prepared in an organic solvent as compared with those prepared by precipitation in an aqueous solvent.

INTRODUCTION

The selective oxidation of *n*-butane is one of the few examples of industrial utilization of a paraffin in heterogeneous catalytic reactions, and therefore is a useful model for studying the characteristics of catalysts able to selectively activate a paraffin. Furthermore, in recent years the use of *n*-butane for the production of maleic anhydride has been considered more favorable as compared to the traditional process from benzene for two principal reasons: (i) economical, since a substantial price difference has developed between benzene and *n*-butane feedstocks, and (ii) environmental, since there are strict controls on benzene emissions, particularly in the United States. These factors make the *n*-butane route most attractive, in spite of the lower productivity of the process from *n*-butane as compared to that from benzene (*1*).

Almost all of the catalysts utilized in industrial plants for the synthesis of maleic anhydride from *n*-butane are vanadium–phosphorus oxide-based catalysts with a phosphorus : vanadium (P : V) atomic ratio near 1.0 (*1*, *2*). However, notwithstanding the academic and scientific effort in recent years on the characterization of this catalytic system (*2–28*), some questions are still open. In particular, a survey of the patent literature (*1*, *2*) indicates a large number of preparation procedures which differ in respect of (i) the solvent utilized (water or an organic solvent), (ii) the starting vanadium compound (such as V_2O_5, NH_4VO_3, or $VOPO_4$), (iii) the reducing agent (HCl, oxalic acid or other organic acids, the organic solvent itself, other reducing agents), and (iv) the P : V ratio and activation procedure. In spite of the great number of parameters varied in the preparation procedures, a general aspect is that the preparations which utilize an organic solvent, either as solvent or both as solvent and reducing agent, lead to catalysts which are more active as compared to those prepared with water as the solvent (*11*, *13*, *17*, *18*, *29–32*). The higher activity has been attributed only to the higher surface area of these catalysts; in all cases always the same active phase [$(VO)_2P_2O_7$] was found to be present.

Recently we reported differences in line

[1] To whom all correspondence should be addressed.

0021-9517/86 $3.00

intensities in the X-ray diffraction patterns of $(VO)_2P_2O_7$ prepared utilizing water or an organic alcohol as the solvent (*13, 17*). Also Bordes *et al.* (*18, 20, 21*), studying the preparation of $(VO)_2P_2O_7$ with different procedures, found different forms of $(VO)_2P_2O_7$ (β- and γ-). Therefore the question is whether or not the higher activities of the vanadium–phosphorus oxide catalysts prepared in an organic solvent derive only from the higher surface areas (*29–32*) or if in these preparations some special type of modification of the catalyst texture and structure occurs which is able to enhance the number of active sites for *n*-butane selective activation.

The aim of the research reported in this paper was to investigate this aspect further, by comparing the structural and catalytic properties of $(VO)_2P_2O_7$ active phases prepared utilizing water or an organic alcohol as the solvent and studying their mechanisms of formation from the $VOHPO_4 \cdot \frac{1}{2}H_2O$ precursor phase (*9, 10, 23*).

EXPERIMENTAL

Catalyst Preparation

a(1) Preparation in aqueous medium. Fifteen grams of V_2O_5 (Carlo Erba RPE) were dissolved in 200 ml of 37% HCl. The solution was boiled and stirred until complete reduction to vanadium(IV) (about 3 h); 19 g of 85% *o*-H_3PO_4 (Carlo Erba RPE) were then added to obtain a P : V atomic ratio of 1.0. This solution was allowed to boil for 2 h and concentrated to 20 ml of solution to which hot water was then added to obtain a blue precipitate. The precipitate was removed from the solution by filtration, washed, and dried at 420 K overnight.

b(1) Preparation in organic medium. Fifteen grams of V_2O_5 (Carlo Erba RPE) were suspended in 90 ml of isobutyl alcohol and 60 ml of benzyl alcohol. The suspension was stirred continuously under reflux for 3 h, then cooled to room temperature and left stirring at this temperature overnight before adding 16.16 g of 99% *o*-H_3PO_4 (Carlo Erba RPE). After the phosphorus addition, the solution was heated and maintained under reflux with constant stirring for 2 h; then the slurry was filtered and, after washing, the filtrate was dried at 430 K for 24 h.

c(1) Catalyst c(1) was prepared in the same way as catalyst b(1), except the solution was not cooled to room temperature before the phosphoric acid solution.

d(1) Catalyst d(1) also was prepared using a method analogous to that for catalyst b(1) except that (i) the time of reduction of the vanadium was shorter (0.5 h), (ii) the reduction was made under nitrogen reflux, (iii) the phosphoric acid was added without cooling of the solution, and (iv) the time under reflux after the addition of the phosphoric acid was longer (6 h).

The following notation has been adopted in this paper: the first letter (a, b, c, or d) indicates the type of preparation, whereas the subsequent number (1 or 2) indicates whether it is the precursor after the drying stage (1), or the active phase after calcination (2).

Catalyst Characterization and Experimental Techniques

The P : V atomic ratio of the catalysts, determined by the method previously reported (*12*), was 1.06 for the sample prepared in an aqueous medium by precipitation [a(1)] and 1.01 for the samples prepared in an organic medium [b(1), c(1), and d(1)]. In all the samples before calcination, the percentage of vanadium(IV) with respect to the total amount of vanadium was 100%. The method used for the chemical analysis of the valence state of vanadium has been reported previously (*14*).

X-Ray diffraction (XRD) analysis (powder technique) was carried out with a Philips diffractometer, using nickel-filtered Cu$K\alpha$ radiation.

Infrared spectra (FT-IR) were obtained using a Nicolet MX 1 Fourier transform infrared spectrometer connected to conventional evacuation ramps and measurements cells.

Differential scanning calorimetry (DSC) and thermogravimetric (TG) data were obtained using a Perkin–Elmer DSC-2 and TG-2 apparatus, respectively, operating under nitrogen flux at a heating rate of 20 K/min.

Scanning electron microscopy (SEM) analysis was performed on a ISO SS40 instrument.

The catalytic tests were carried out in a tubular isothermal flow reactor (*15*) at atmospheric pressure. The effluent, kept at 450 K to prevent condensation of the products, was analyzed by gas chromatography and then, after cooling to room temperature, was analyzed a second time by gas chromatography to determine noncondensable gas. Further details of this method have been reported elsewhere (*15, 16*). Before the catalytic tests, the catalysts were conditioned in a flow of the reacting mixture (1% *n*-butane/air) for 3 h at the reaction temperature for the tests. After this time, no changes in activity or selectivity were noted in about 3 days of working time. The tests to verify the absence of diffusion phenomena have been reported elsewhere (*15*). All catalytic tests were carried out with the following gas composition: 0.56% *n*-butane, 11.6% oxygen, and 87.4% nitrogen.

RESULTS

X-Ray Diffraction (XRD)

Figure 1 shows the XRD patterns of the precursor of the active phase prepared in an aqueous medium [a(1)] and in an organic medium [b(1) → d(1)]. In samples b → d, the method of adding the phosphoric acid was varied according to the procedures given in the experimental section. All preparation methods gave only the same compound, corresponding to $VOHPO_4 \cdot \frac{1}{2}H_2O$ (*9, 10, 20, 23*), but only the precursor prepared in an aqueous medium by precipitation [a(1)] shows line intensities which correspond well to that of $VOHPO_4 \cdot \frac{1}{2}H_2O$. In the precursors prepared in an organic medium [b(1) → d(1)] disorder always is

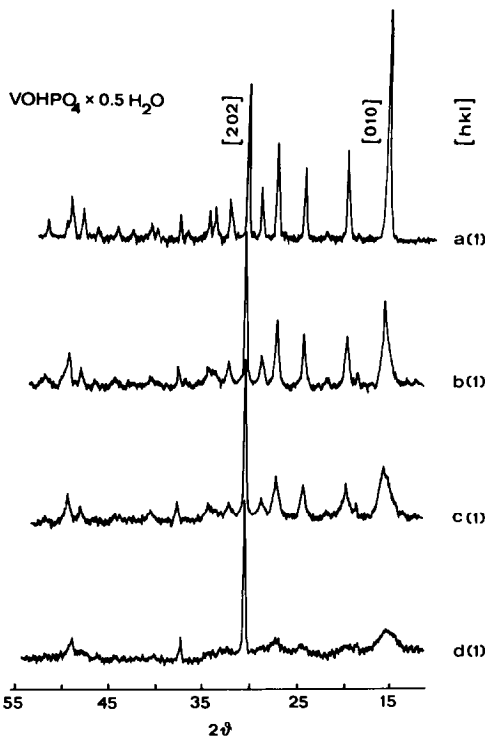

FIG. 1. X-Ray diffraction patterns of precursors.

present along the (010) plane, as shown by the width of the (010) reflection as compared with that of the (202) reflection. The XRD reflections are indexed according to Bordes *et al.* (*20*); due to a different space group for the $VOHPO_4 \cdot \frac{1}{2}H_2O$, Johnson *et al.* (*9*) have reported a different (*hkl*) index for the same XRD diffraction line.

Depending on the method of preparation it is possible to obtain precursors with different degrees of disorder along the (010) plane [b(1) → d(1)]. The possibility that the observed broadening of the (010) reflection derives from the presence of other compounds either of V(V) or of V(IV) with a P:V ratio higher than 1.0, such as the $VO(H_2PO_4)_2$ found by Hutchins and Higgins (*33*), can be excluded on the basis of the chemical analysis of the b(1), c(1), and d(1) samples which had a P:V ratio of 1.0 and 100% of V(IV). Furthermore, neither the XRD reflections nor the IR bands characteristic of $VO(H_2PO_4)_2$ (*34*) are present in our case.

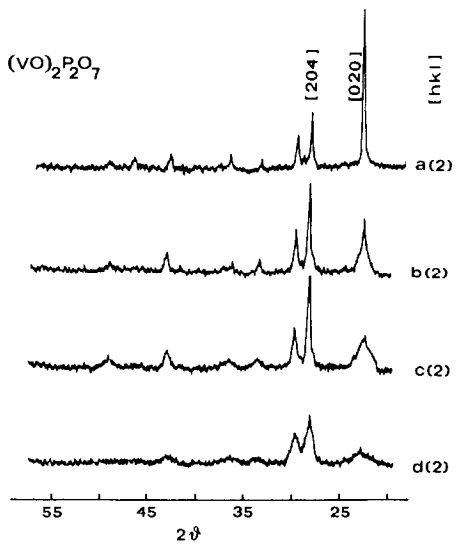

FIG. 2. X-Ray diffraction patterns of active phases.

Figure 2 shows the XRD patterns of the same compounds of Figure 1 after calcination at 670 K (3 h) in a mixture of 1% *n*-butane/air to limit the formation of crystalline $VOPO_4$. As before, all preparations gave the same compound corresponding to $(VO)_2P_2O_7$ (*19*, *22*), but only in the sample prepared in an aqueous medium did the intensities of the diffraction peaks correspond to those reported by Bordes and Courtine (*19*) and Gorbunova and Linde (*22*) for $(VO)_2P_2O_7$. The preparations in an organic medium all gave disorder along the (020) plane as indicated by the different peak widths of the (020) and (204) reflections. The degree of disorder depends on the method of preparation, but the same sequence of degree of disorder was found in the precursor and in the active phase, i.e., the most deformed precursor structure gave the most deformed active phase.

Fourier Transform Infrared Spectra (FT-IR)

The absorption bands of the $VOHPO_4 \cdot \frac{1}{2}H_2O$ [sample b(1)] and, for comparison, the $(VO)_2P_2O_7$ [sample b(2)], are reported in Table 1. Assignments were made on the basis of the structure reported by Torardi and Calabrese (*23*) and by Johnson *et al.* (*9*, *10*), and by comparison with the spectra of compounds having similar structural units such as: (i) metal hydrogen and dihydrogen phosphates (*35*, *36*), (ii) other V(IV)=O salts (*37*, *38*), and (iii) other bridged aquometal complexes (*39*, *40*). Based on this spectrum, which has been reported previously (*12*), further considerations on this structure can be made. In general, all spectroscopic features agree with a very weak bonding between the layers containing V—O—P bonds which constitute the 0*K*0 family of planes. In fact, the very low frequency of the P—OH in-plane deformation, and the high value corresponding to ν(PO)—H (probably identified as a broad absorption superimposed on νOH of water), certainly greater than 3050 cm^{-1},

TABLE I

Infrared Spectra of $VOHPO_4 \cdot \frac{1}{2}H_2O$ and $(VO)_2P_2O_7$. Absorption Bands (cm^{-1}) and Vibration Assignments

$VOHPO_4 \cdot \frac{1}{2}H_2O$[a]		$(VO)_2P_2O_7$	
3590	$\nu_a OH_2$		
3370	$\nu_s OH_2$		
3050	ν(P)—OH		
2320	$\delta H_2O + \omega H_2O$	2445	$2 \times \nu_{as}PO_3$
2240	$2 \times \nu_a PO_3$	2300	$\nu_{as} + \nu_s PO_3$
		2230	$2 \times \nu_{as}PO_3$
2015	$\nu_a + \nu_s PO_3$	1995	$\nu_{as}PO_3 + \nu_s$POP
1985	$2 \times \nu_s PO_3$	1940	$2 \times \nu$V=O
1950	$2 \times \nu$V=O	1865	$\nu PO_3 + \nu$POP
1818	δ_{ip}POH + δ_{oop}POH		
1645	δH_2O		
1132	δ_{ip}POH	1235	$\nu_{as}PO_3$
1194	$\nu_{as}PO_3$	1220	
1103		1140	$\nu_{as}PO_3$
1050		1115	
976	νV=O (+$\nu_s PO_3$)	1095	$\nu_s PO_3$
930	νP—(OH)	966	νV=O
686	ωH_2O	960	ν_{as}POP
641	δ_{oop}POH	792	νV—(O=V)
		740	ν_sPOP
548	δ OPO	627	δ OPO
531		577	
483		504	
416		420	

[a] On the basis also of the IR spectrum of $VODPO_4 \cdot \frac{1}{2}D_2O$ reported by Johnson *et al.* (*9*).

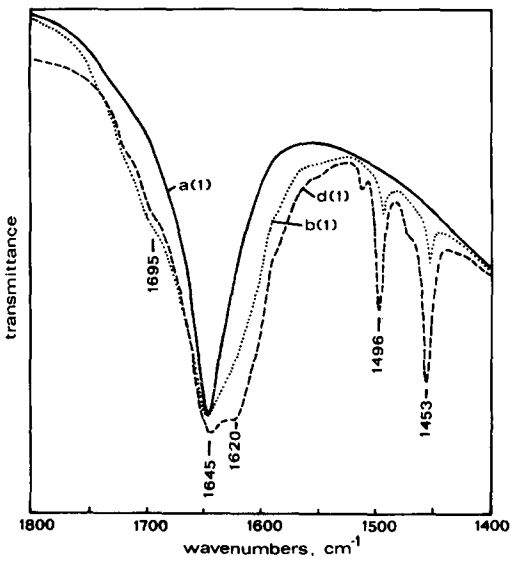

FIG. 3. FT-IR spectra of precursors in the region 1400–1800 cm^{-1}.

clearly indicate that H-bonding involving hydrogen-phosphate ions is very weak. Correspondingly, the νV=O frequency is relatively high, indicating a poor perturbation. This agrees with the short O—H bond characterizing this structure (*23*). Water molecules also appear not be involved in strong H-bonding.

The spectra of the precursors prepared in aqueous and organic media do not differ greatly in the region 1300–1500 cm^{-1}, where skeletal vibrations fall. Only slight differences in the shape of some bands are observed, confirming that they are substantially formed by the same crystalline compound. However, relevant differences may be observed at higher frequencies. Reported in Fig. 3 are the spectra (KBr pressed disks in dry atmosphere) of such compounds, after calcination at 423 K for 36 h, in the 1800- to 1400-cm^{-1} region. The precursor prepared in an aqueous medium [a(1)] shows a single sharp band centered at 1645 cm^{-1}. Such a frequency is typical of coordinated water (in-plane deformation) in agreement with the crystal structure. This band disappears in samples calcined near 670 K, leaving a broader and less intense band near 1620 cm^{-1}. This band also is found in pressed disks of pure compound (KBr not added) and disappears by evacuation near 670 K. This behavior is due to the decomposition of $VOHPO_4 \cdot \frac{1}{2}H_2O$ to produce $(VO)_2P_2O_7$ (as indicated clearly by the skeletal frequency region), which retains part of the water in a reversible adsorbed form. In the spectra of the precursors prepared in organic medium [Fig. 3, samples b(1) and d(1), characterized by an increased disorder along the (010) plane], shoulders both in the higher and lower frequency sides of this band are observed, namely at 1695 and 1620 cm^{-1}. The last component, probably related to uncoordinated hydrogen-bonded water, is particularly intense in spectrum d(1), which is characterized by higher disorder. In samples b(1) and d(1) then, more than one type of water is present in the crystals. However, samples prepared in an organic medium also show sharp bands at 1496 and 1453 cm^{-1}, very intense in precursor d(1). During heating also in a nitrogen atmosphere, such bands disappear, but an intense band simultaneously appears at 2345 cm^{-1}, typical of nonrotating trapped CO_2 molecules. The bands at 1496 and 1453 cm^{-1} may be attributed to residual benzyl alcohol [19a and 19b phenyl ring vibrations, according to the Wilson notation (*41*)] which burns during calcination to produce CO_2. In confirmation, weak bands at 3090, 3065, and 3030 cm^{-1}, typical of aromatics (νCH) also are observed in sample d(1).

Figure 4 shows the FT-IR spectra of the active phases prepared in aqueous and organic media, obtained from precursors a(1), b(1), and d(1) by heating in nitrogen at 670 K. Only small differences are found between samples a(2) and b(2), namely, in the sample prepared in organic medium [b(2)], the shoulders at 1285, 1005, 930, 915, 790, 700 cm^{-1} and the band at 570 cm^{-1} are absent. However, substantially the spectra imply the same crystalline compound. On the contrary, the spectrum of sample d(2) is poorly resolved and XRD analysis indicates

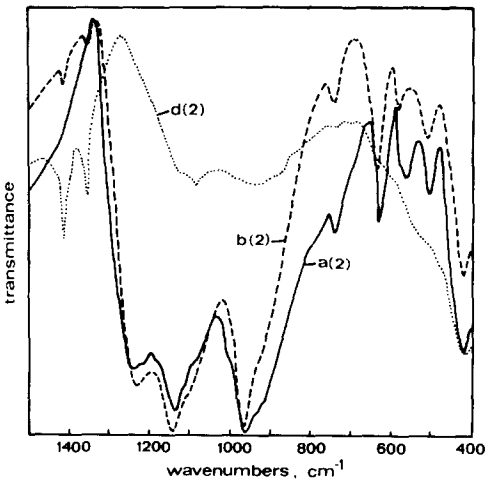

FIG. 4. FT-IR spectra of vanadium–phosphorus oxide samples after heating in a nitrogen atmosphere at 670 K.

that it is XRD amorphous. After heating in nitrogen at 670 K for 4 h, organic alcohol is still present in sample d(2) (Fig. 4). In sample b(2), after heating in the same conditions, these bands also are present, but are much less intense.

Figure 5 reports the FT-IR spectra of the active phases prepared in aqueous and organic media after the catalytic tests (*n*-butane oxidation) and of $VOPO_4 \cdot 2H_2O$ (spectrum e) for comparison. It is worth noting that in all cases, XRD analysis detects only

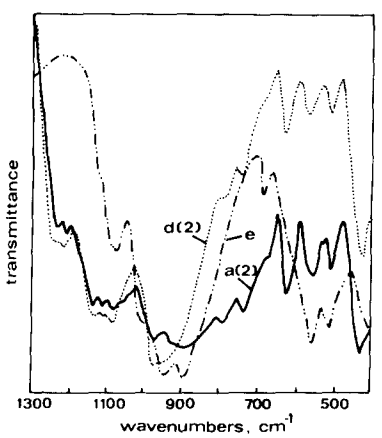

FIG. 5. FT-IR spectra of vanadium–phosphorus oxide samples after catalytic runs (*n*-butane oxidation) and of $VOPO_4 \cdot 2H_2O$ (spectrum e).

the $(VO)_2P_2O_7$ phase in the catalyst, oxidized phases not being observed. On the contrary, large differences are observed in infrared spectra. The spectrum of sample b(2) is the same as after heating in a nitrogen atmosphere. Assignments of the bands are reported in Table 1 according to the spectra of other metal pyrophosphates. On the contrary, in the samples a(2) (aqueous medium) and d(2) (organic medium with highly disordered structure), after catalytic tests other bands (namely at 1075, 910, and 676 cm^{-1}, assigned to the hydrated form of α-$VOPO_4$ and corresponding to the more intense vibrations of $VOPO_4 \cdot 2H_2O$ (spectrum e) prepared according to Ladwig (*42*) also are observed. The observation of V(V) is confirmed by chemical analysis where the amount of V(V) with respect to the amount of total vanadium is 15, 0, and 10% for samples a(2), b(2), and d(2), respectively.

In conclusion, the FT-IR data, in good agreement with chemical analysis, indicate that sample b(2) after catalytic runs is only $(VO)_2P_2O_7$, while in both samples a(2) and d(2) an oxidized phase ($VOPO_4 \cdot nH_2O$) is present together with the vanadyl pyrophosphate.

Differential Scanning Calorimetry (DSC) and Thermogravimetric (TG) Analyses

Figure 6A shows the DSC results (heating rate 20 K/min in nitrogen) for the transformation

$$VOHPO_4 \cdot \tfrac{1}{2}H_2O \rightarrow (VO)_2P_2O_7 + 2H_2O$$

on the same precursors as shown in Fig. 1. Before DSC analysis, the samples were preconditioned at 423 K in nitrogen to constant weight in order to remove adsorbed species. The corresponding TG curves are reported in Fig. 6B.

In the precursor prepared in an aqueous medium by precipitation [a(1)], both DSC and TG analyses show that the transformation occurs at high temperatures and in a single step. The weight loss corresponds well to the theoretical weight loss of two

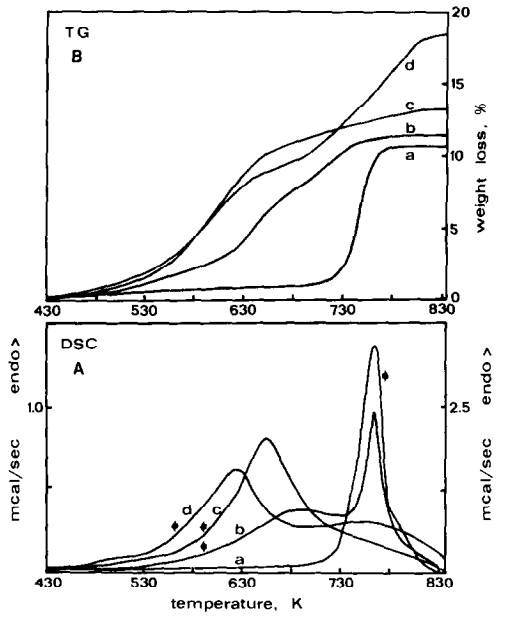

FIG. 6. DSC (A) and TG (B) curves (nitrogen atmosphere; heating rate 20 K/min) of precursors.

water molecules (10.5%). On the contrary, for the samples prepared in an organic medium, the transformation occurs over a broader range of temperatures and starts at much lower temperatures. The total weight is higher than that of the sample prepared in an aqueous medium and increases from sample b(1) to sample d(1), in good agreement with the previously shown increase in the amount of alcohol retained inside the structure. Two stages of the transformation can be distinguished in the samples prepared in an organic medium; in fact the DSC curves derive from the superimposition of a sharp peak on a broader peak. The temperature of the maximum of the sharper peak (see Fig. 6) decreases in the order b(1) → d(1), in agreement with the increasing disorder of the structure of the samples.

IR analysis of the catalysts after the maximum of the sharper peak suggests that this peak is associated with the loss of crystallization water, whereas the broader peak is associated with the loss of water deriving from the condensation of two hydrogenphosphate groups.

TG isothermal experiments in a nitrogen atmosphere at 670 K (Fig. 7) indicate that after about 50 min, none of the samples lose further weight. The rate of weight loss increases from sample a(1) to sample d(1), in good agreement with the results from temperature scanning (see Fig. 6b). IR analysis (see Fig. 4) after the isothermal experiments indicates that the transformation to vanadyl pyrophosphate is complete. However, in the samples prepared in an organic medium, organic alcohol is still present and can be removed only by further heating at higher temperatures (770 K), as indicated both from TG and IR analyses. In isothermal experiments in air at 670 K, on the contrary, after 50 min the bands due to organic alcohol completely disappeared in all samples prepared in an organic medium. Furthermore, after the isothermal heating at 670 K in nitrogen atmosphere, the chemical analyses of the samples prepared in an organic medium indicate a reduction of the vanadium [6% of V(III) found in sample b], not present in the sample prepared in an aqueous medium. This suggests that in the absence of oxygen, the process of alcohol release from the catalyst structure is very slow and that also a slight amount of organic alcohol can be retained in the vanadyl pyrophosphate structure.

Figure 8 shows the rate of oxidation (in air at 670 K) of vanadium(IV) to V(V) for $(VO)_2P_2O_7$ prepared in an aqueous medium by precipitation [a(2)] and prepared in an

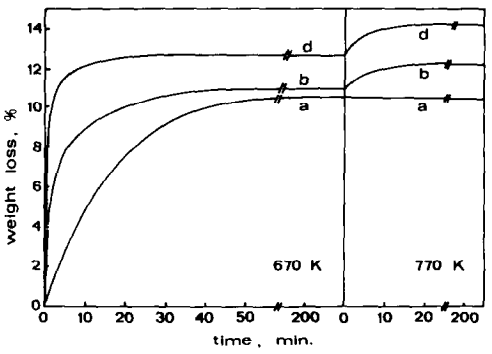

FIG. 7. TG isotherms (nitrogen flow) of precursors.

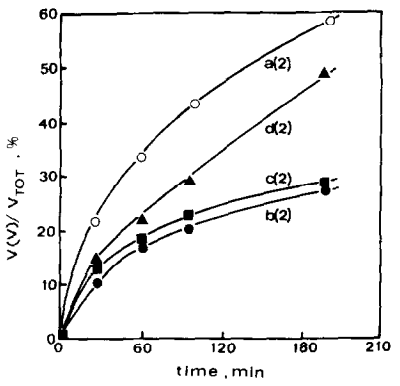

FIG. 8. Rate of vanadium(IV) oxidation to vanadium(V) (temperature 670 K; air flow) of active phases.

organic medium with different degrees of disorder [b(2) → d(2)]. The active phase prepared in an aqueous medium shows a higher rate of oxidation of vanadium(IV) as compared with that for the active phase prepared in an organic medium. However, the degree of disorder of the structure also influences the rate of vanadium(IV) oxidation; the lower rates of vanadium(IV) oxidation are found for samples b(2) and c(2), whereas sample d(2) shows a higher rate of vanadium(IV) oxidation.

Scanning Electron Microscopy (SEM)

Figure 9 reports SEM micrographs of the precursor catalysts prepared in an aqueous solvent [a(1)] and in an organic solvent [b(1) and d(1)]. In contrast to sample a(1), samples prepared in an organic solvent clearly show a lamellar morphology with well-formed plate-like crystals; in agreement with XRD results, the lamellar morphology is more accentuated in sample d(1).

After the transformation to vanadyl pyrophosphate [samples a(2) and b(2)], the difference in morphology between the aqueous [a(2)] and organic [b(2)] preparations still remains. In particular, a lamellar morphology in sample b(2) is still present, although less evident than in the precursor samples.

Catalytic Data

Figure 10 reports the comparison between the specific rate (per m^2 of surface area of the catalyst) of maleic anhydride formation from *n*-butane and from 1-butene for active phases prepared in an aqueous medium [a(2)] and in an organic medium [b(2)]. The preparation in an organic medium is more active than the preparation in an aqueous medium which is active only at temperatures about 100 K higher. Furthermore, considering also the different surface areas of the two catalysts (27 and 5.6 m^2/g for samples b(2) and a(2), respectively), the difference in activity becomes more relevant.

Figure 11A reports the yields of maleic anhydride versus conversion (at 530 K) in *n*-butane selective oxidation for the samples b(2), c(2), and d(2) prepared in an organic medium. Figure 11B reports the curves of conversion versus W/F. Sample d(2), which has the more deformed XRD pattern, is the less active (see Fig. 11B) and the less selective at high conversion (see Fig. 11A), but is of comparable selectivity in maleic anhydride formation at low conversion. However, it is more active as compared with the preparation in an aqueous medium. No great differences either in activity or selectivity were found for the two samples b(2) and c(2), although the better results are obtained with sample b(2).

DISCUSSION

Structure of Precursor of Active Phase

Recently several authors (*9, 10, 20–23*) have determined the structure of the precursor of the active phase and have indicated that it is a hydrated vanadyl hydrogen phosphate [$VOHPO_4 \cdot \frac{1}{2}H_2O$] formed by vanadyl hydrogen phosphate layers stacked along the *c* axis. The plane passing through the layer is the (010) plane in agreement with the indices of XRD reflections reported by Bordes *et al.* (*20, 21*). The infrared spectrum of the precursor (Table 1) agrees with this structural determination,

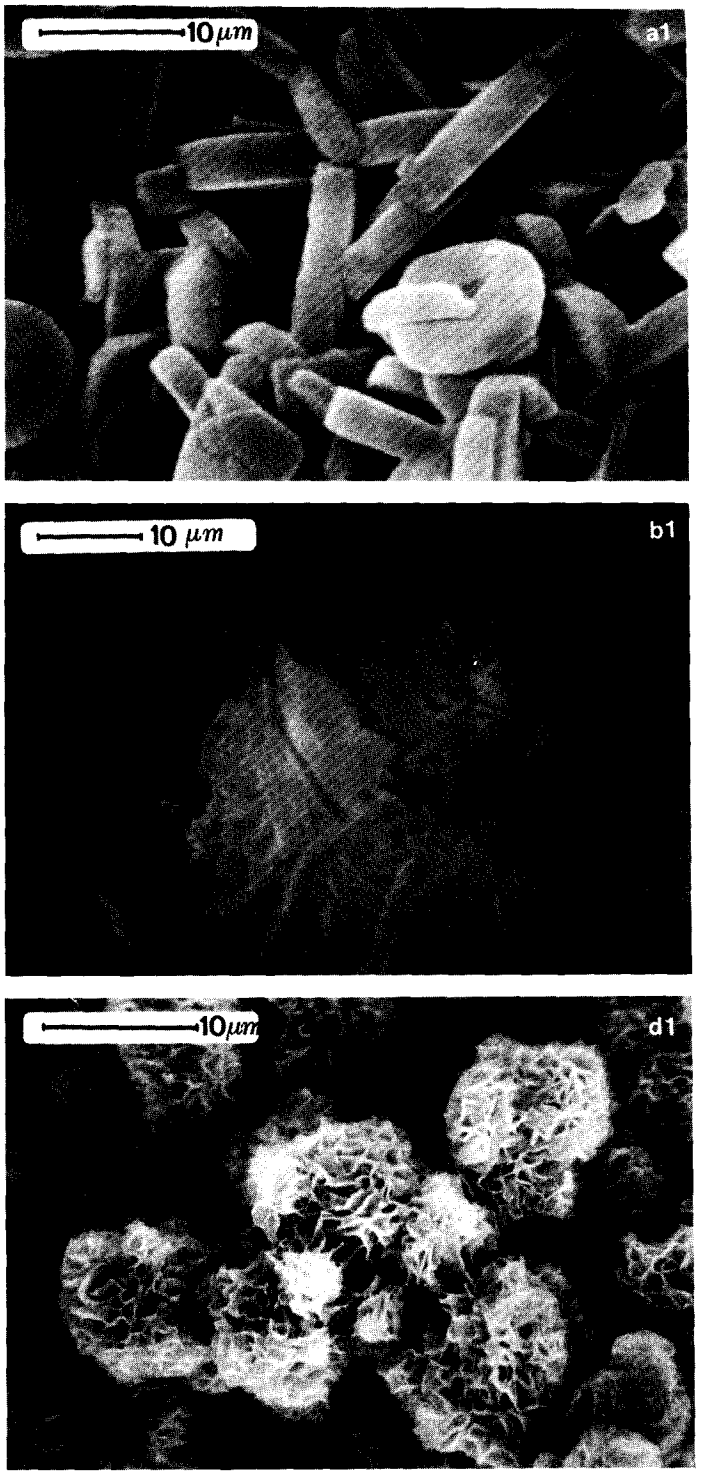

FIG. 9. SEM micrographs of precursors (A) and of active phases (B): a(1) ×2320; b(1) ×1630; d(1) ×2460; a(2) ×1500; b(2) ×3680.

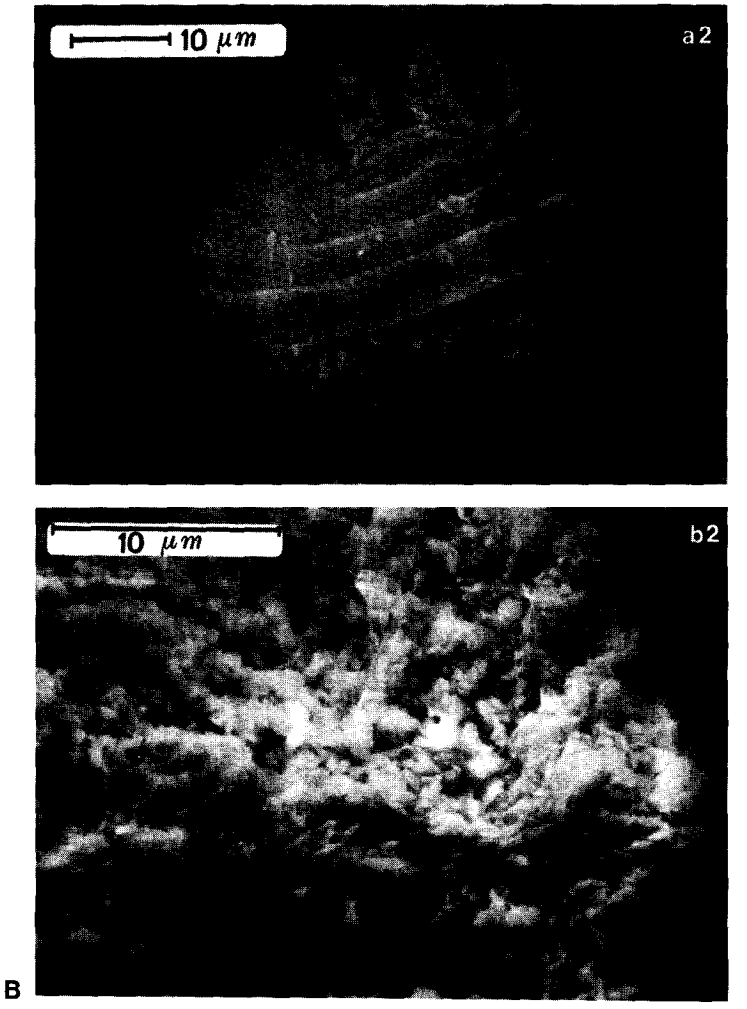

FIG. 9—*Continued.*

but indicates that the band of P—OH bending occurs at lower frequency (1132 cm^{-1}) than that usually found for hydrogen phosphates (*35, 36*). For this reason we previously suggested a pyrophosphate structure for the precursor of the active phase (*5, 8*), since a band centered near 1200 cm^{-1} is typical of pyrophosphates (*43, 44*). However, the low frequency of the P—OH in-plane deformation indicates a short O—H bond length and therefore no strong hydrogen bonds between the layers. In fact, organic alcohols can be easily trapped between the layers, as indicated by thermal analysis (Fig. 6) and by FT-IR spectra (Fig. 3). Further evidence of the presence of a deformed crystalline structure in the catalysts prepared in an organic medium derive from the different shapes of the bands in infrared spectra corresponding to crystallization water (Fig. 3), which indicate only one type of crystallization water in the highly crystalline precursor prepared in an aqueous medium [a(1)] and additional types of crystallization water in the catalysts prepared in an organic medium. These data agree with XRD analysis, which showed that the catalysts prepared in an organic medium were disordered along the (010) plane.

All data indicate, therefore, that it is possible to obtain, depending on the method of preparation, a $VOHPO_4 \cdot \frac{1}{2}H_2O$ structure

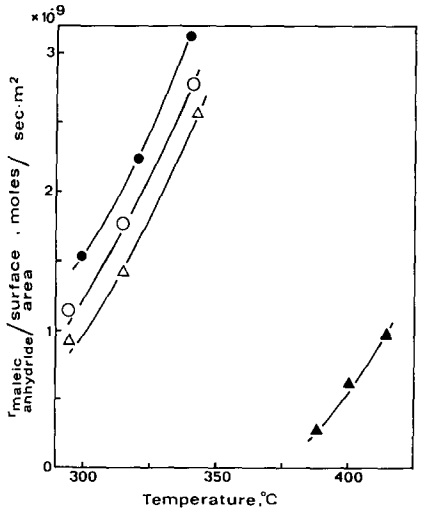

FIG. 10. Comparison of the specific rate (per m^2 of surface area of the catalyst) of maleic anhydride formation from *n*-butane (full symbols) and from 1-butene (open symbols) as a function of the reaction temperature for active phases prepared in an aqueous medium [a(2): (△▲)] and in an organic medium [b(2): (○●)].

with different degrees of disorder between the stacked planes, where the organic alcohols utilized as reducing agents in the preparation in an organic medium can be trapped.

The structure of the vanadyl hydrogen phosphate suggests a direct analogy with the layered structure of the hydrogen phosphates of zirconium and titanium (*45*). In particular, it has recently been found that these compounds could be pillared by organic phosphates and phosphonates, where the P—OH group of the acid phosphate is replaced by the P—R group of an organophosphonate or the P—OR group of an organophosphate (*46*). However, in this case, the interlayer spacing is two times higher than the interlayer spacing of vanadyl hydrogen phosphate, suggesting that our case is not a pillared compound, but rather only a deformation in the length of the stacked layers induced by the presence of trapped organic alcohol which is not directly involved in bonds with the inorganic phosphate. This interpretation also agrees with recent results on vanadyl organophosphonates (*47*); in these compounds different structures are found and in particular there is little indication of V^{4+}–V^{4+} magnetic interaction (*47*). In contrast, the corresponding data for vanadyl hydrogen phosphate show pairwise antiferromagnetic exchange interactions arising from the presence of bridged vanadium(IV) pairs in the structure (*47*). This confirms the difference between the two structure types, a deformed $VOHPO_4 \cdot \frac{1}{2}H_2O$ structure and the vanadyl organophosphonates.

Topotactic Transformation of the Precursor of the Active Phase

The strong differences between the loss of water (Fig. 6) for the two preparations in aqueous [a(1)] and in organic media [b(1) → d(1)], indicate that the presence of disorder along the plane of stacking of the layers drastically modifies the mechanisms of wa-

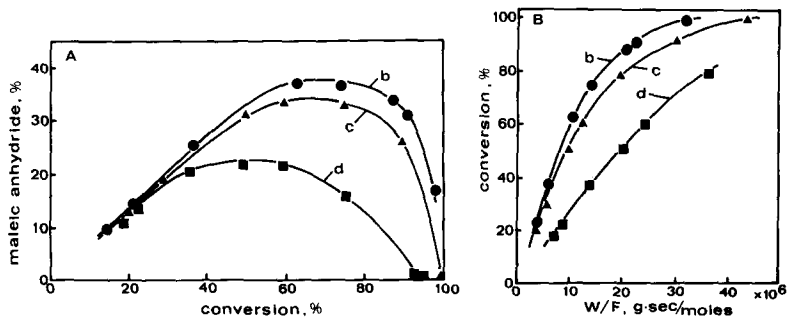

FIG. 11. Maleic anhydride yield versus conversion (A) and conversion versus W/F (B) at 580 K for various active phases prepared in an organic medium.

ter loss and condensation of phosphate groups. The increasing degree of disorder along the (010) plane [from sample b(1) to d(1)], increases the rate of dehydration (Fig. 7). A comparison between sample b(1) and d(1), which have similar surface areas (10 and 9 m^2/g, respectively) indicates that the rate of dehydration is strongly affected by the morphology of the catalyst (Fig. 9) in agreement with the change in the mechanism of the transformation to the active phase as suggested by Bordes *et al.* (*20, 21*). Furthermore, the presence of organic material trapped between the layers also modifies the mechanism of the transformation. As indicated by Figs. 4 and 5, for sample d(1), the transformation to the active phase does not occur in the absence of gaseous oxygen, due probably to the removal of lattice oxygen during the release of alcohol as CO_2 from the catalyst which destroys the catalyst structure (XRD amorphous, and IR spectrum very poorly resolved). According to this interpretation, the process of alcohol release in the absence of gaseous oxygen is a very slow process (Fig. 7) and after the transformation the catalysts are reduced.

The texture of the precursor not only influences the solid state transformation to the active phase, but also the nature of the texture of the active phase obtained. A comparison between Figs. 1 and 2 clearly indicates that a highly crystalline precursor leads to a well crystallized $(VO)_2P_2O_7$, whereas precursors showing disorder along the cleavage plane lead to active phases with comparable disorder on the same cleavage plane [(010) and (020), respectively]. SEM micrographs of the precursors and active phases support this interpretation, and further indicate that the transformation from $VOHPO_4 \cdot \frac{1}{2}H_2O$ to $(VO)_2P_2O_7$ is a topotactic reaction, as suggested by Bordes *et al.* (*20, 21*) and Johnson *et al.* (*9*).

Nature of the Active Phase

The structure of the active phase [$(VO)_2P_2O_7$] has been determined by Bordes and Courtine (*19*) and Gorbunova and Linde (*22*). The vanadyl pyrophosphate structure is a three-dimensional network formed by vanadyl phosphate layers along the *c* direction joined together by pyrophosphate groups. During the transformation

$$VOHPO_4 \cdot \tfrac{1}{2}H_2O \rightarrow (VO)_2P_2O_7 + 2H_2O$$

due to loss of crystallization water, the dimer vanadyl groups shift to a parallel position and after condensation of the hydrogen phosphate groups, a rearrangement from *cis* to *trans* vanadyl occurs (*23*). The transformation involves only breaking of $V—OH_2$ and $P—(OH)\cdots H$ bonds and leaves the V—O—P connections intact. Therefore the texture of the active phase is pseudomorphic with that of the initial precursor structure, as clearly indicated by Figs. 1 and 2 and by SEM micrographs. Therefore, although the vanadyl pyrophosphate has a three-dimensional structure, it is possible to induce some disorder in the structure via the precursor texture.

Influence of the Texture on Redox Properties

The texture of the catalyst considerably influences the redox properties of the catalysts. Figure 8 shows that disorder along the (020) plane [samples b(2) and d(2) as compared with sample a(2)] considerably reduces the rate of oxidation of vanadium(IV) to vanadium(V), although the more highly disordered structures are easier to oxidize than the less disordered ones [samples d(2) and b(2), respectively]. Furthermore, Fig. 5, in agreement with the data from chemical analysis, shows that after the catalytic tests (all after the same cycle of catalytic runs), only sample b(2) has the infrared spectrum of pure $(VO)_2P_2O_7$. Samples d(2) and a(2), more easily oxidizable, both present bands due to vanadium(V)-phosphate [$VOPO_4$], more intense in the sample prepared in an aqueous medium.

In a previous paper (*13*), in agreement

also with other authors (*25, 28*), we indicate that the stabilization of vanadium(IV) with respect to its oxidation to V(V) is an important factor determining the catalytic properties in *n*-butane oxidation. A high rate of V(IV) oxidation to V(V) causes over-oxidation of the surface of the catalyst, especially in the zone of the catalytic bed corresponding to high conversion where the oxidizing power of the reactant mixture is greatest (*15*). The over-oxidation of the catalyst surface considerably enhances the rate of the successive reaction to carbon oxides of the maleic anhydride formed (*16*), drastically decreasing the yield of maleic anhydride. This explains the different selectivities at high conversion between sample b(2) and d(2).

Influence of the Structure on Catalytic Properties

Figure 10 shows that the preparation in an organic medium is more active than that obtained in an aqueous medium, also considering the specific rate per square meter of surface area of the catalysts. Furthermore, the surface area is higher in the preparation in an organic medium (*12*) and therefore the real activity in *n*-butane selective oxidation (per gram of catalyst) is much higher. The catalysts prepared in an organic medium are all active, but slight variations are found (Fig. 11) depending on the nature of the texture of the active phase. The best results in *n*-butane selective oxidation are obtained with a catalyst whose structure is intermediate between the well crystallized structure of sample a(2) [preparation in an aqueous medium] and the structure of sample d(2) [preparation in an organic medium highly disordered along the (020) plane]. On the contrary, no great differences in the specific rate of 1-butene selective oxidation to maleic anhydride are found between the preparations in aqueous and organic media. The first step of the mechanism of *n*-butane selective oxidation to maleic anhydride is its oxidative dehydrogenation to an intermediate, which in particular conditions that avoid its successive oxidation, can desorb as butenes (*14*). The considerable influence of the texture of the catalyst on the rate of *n*-butane and not on the rate of 1-butene selective oxidation, suggests that the specific nature of the active phase mainly influences this first step of paraffin selective activation. It is worth noting that all catalysts prepared in an organic medium are much more active in *n*-butane oxidation than the sample prepared in an aqueous medium. This suggests that in these catalysts some special modifications of the structure are induced by the presence of the alcohol between the layers during the calcination stage. As previously indicated, the precursor → active phase transformation is a topotactic reaction which involves the *cis* → *trans* electronic rearrangement of the dimer vanadyl groups to form the $(VO)_2P_2O_7$ idealized structure reported in Fig. 12. During this transformation the presence of organic material between the layers can provoke some local defect structures by steric hindrance or as a consequence of oxygen vacancies caused by the reaction of the alcohol with the structural oxygen to form carbon oxides. We think, therefore, that disorder in this plane may derive from the presence of a defect structure, i.e., one of the possibilities shown in Scheme 1. The disorder along the (020) plane can derive from a missing oxygen atom, from the inversion from a *trans* to a *cis* vanadyl position, or from the modification of the V—O bond strength. In any case, this defective

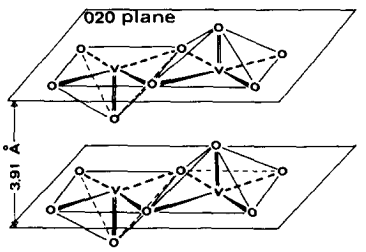

FIG. 12. Idealized $(VO)_2P_2O_7$ structure (only vanadyl octahedra).

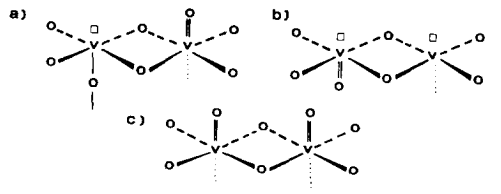

SCHEME 1. Possible local structural modifications of the $(VO)_2P_2O_7$ structure.

structure leads to the formation of a highly reactive pair of vanadium ions, able to activate the paraffin with a coordinative attack. In fact, the V–V distance (about 3.33 Å) corresponds well with the distance necessary to interact with the hydrogens linked to C_1 and C_3 atoms of *n*-butane.

CONCLUSIONS

The use of an organic alcohol as a reducing agent instead of hydrochloric acid leads to the formation of a vanadyl phosphate ($VOHPO_4 \cdot \frac{1}{2}H_2O$) with the organic alcohol trapped between the layers forming the structure of the phosphate. During the succeeding heating, the hydrogen phosphate topotactically transforms, through the loss of two water molecules, to a vanadyl pyrophosphate [$(VO)_2P_2O_7$] pseudomorphic to the initial texture of the precursor. It is thus possible to obtain $(VO)_2P_2O_7$ catalysts with disorder in the plane of layer stacking. Disorder in the (020) plane considerably influences: (i) the catalytic activity in *n*-butane selective activation and (ii) the redox properties of the catalyst, both modifying the rate of vanadium(IV) oxidation to V(V) and the reducibility of the catalyst in a flow of 1% *n*-butane/air. In all the catalysts prepared in an organic medium the specific rate of *n*-butane oxidation is higher than that of the catalysts prepared in an aqueous medium, whereas no great differences are found in the oxidation of 1-butene, the intermediate in the mechanism of maleic anhydride formation from *n*-butane. The organic alcohol trapped between the layers during its removal from the phosphate structure creates local modifications, inducing the formation of new active centers for the activation of *n*-butane, which is the rate-limiting step in the *n*-butane → maleic anhydride reaction.

ACKNOWLEDGMENTS

Support of this work from "Progetto Finalizzato Chimica Fine" of the National Research Council (Rome) is gratefully acknowledged. The authors thank Professor V. Lorenzelli (University of Genova, Italy) for valuable suggestions and for use of the FT-IR spectrometer and Mr. F. Fenu for making the SEM micrographs.

REFERENCES

1. Wohlfahrt, K., and Emig, G., *Hydrocarbon Process* **6,** 83 (1980).
2. Hodnett, B. K., *Catal. Rev.-Sci. Eng.* **27,** 373 (1985).
3. Varma, R. L., and Saraf, D. M., *Ind. Eng. Chem. Prod. Res. Dev.* **18,** 7 (1979).
4. Moser, T. P., and Shrader, G. L., *J. Catal.* **92,** 216 (1985).
5. Poli, G., Resta, I., Ruggeri, O., and Trifirò, F., *Appl. Catal.* **1,** 395 (1981).
6. Centi, G., Manenti, I., Riva, A., and Trifirò, F., *Appl. Catal.* **9,** 177 (1984).
7. Morselli, L., Trifirò, F., and Urban, L., *J. Catal.* **75,** 395 (1981).
8. Centi, G., Galassi, C., Manenti, I., Riva, A., and Trifirò, F., *in* "Preparation of Catalysts III" (G. Poncelet *et al.*, Eds.), Vol. 16, p. 542. Elsevier, Amsterdam, 1983.
9. Johnson, J. W., Johnston, D. C., Jacobson, A. J., and Brody, J. F., *J. Amer. Chem. Soc.* **106,** 8123 (1984).
10. Leonowicz, M. E., Johnson, J. W., Brody, J. F., Shannon, H. F., and Newsam, J. M., *J. Solid State Chem.* **56,** 370 (1985).
11. Cavani, F., Centi, G., and Trifirò, F., *Ind. Eng. Chem. Prod. Res. Dev.* **22,** 570 (1983).
12. Cavani, F., Centi, G., and Trifirò, F., *Appl. Catal.* **9,** 191 (1984).
13. Cavani, F., Centi, G., Manenti, I., and Trifirò, F., *Ind. Eng. Chem. Prod. Res. Dev.* **24,** 221 (1985).
14. Centi, G., Fornasari, G., and Trifirò, F., *J. Catal.* **89,** 44 (1984).
15. Centi, G., Fornasari, G., and Trifirò, F., *Ind. Eng. Chem. Prod. Res. Dev.* **24,** 32 (1985).
16. Cavani, F., Centi, G., and Trifirò, F., *Appl. Catal.* **15,** 151 (1985).
17. Cavani, F., Centi, G., and Trifirò, F., *J. Chem. Soc. Chem. Commun.*, 492 (1985).
18. Bordes, E., and Courtine, P., *J. Chem. Soc. Chem. Commun.*, 294 (1985).
19. Bordes, E., and Courtine, P., *J. Catal.* **57,** 236 (1979).

20. Bordes, E., Courtine, P., and Johnson, J. W., *J. Solid State Chem.* **55,** 270 (1984).
21. Bordes, E., Courtine, P., and Johnson, J. W., *in* "Proceedings, 10th International Symposium on the Reactivity of Solids" (Dijon, 1984), p. 502. Elsevier, Amsterdam, 1985.
22. Gorbunova, Yu. E., and Linde, S. A., *Sov. Phys.-Dokl. (Eng. Transl.)* **24,** 138 (1979).
23. Torardi, C. C., and Calabrese J. C., *Inorg. Chem.* **23,** 1308 (1984).
24. Hodnett, B. K., and Delmon, B., *J. Catal.* **88,** 43 (1984).
25. Hodnett, B. K., and Delmon, B., *Ind. Eng. Chem. Fundam.* **23,** 465 (1984).
26. Hodnett, B. K., Permanne, Ph., and Delmon, B., *Appl. Catal.* **6,** 231 (1983).
27. Hodnett, B. K., and Delmon, B., *Appl. Catal.* **9,** 203 (1984).
28. Hodnett, B. K., and Delmon, B., *Appl. Catal.* **15,** 141 (1985).
29. Schneider, R.A., U.S. Patent 4,043,943 (1977).
30. Katsumoto, K., and Marquis, D. M., U.S. Patent 4,132,670 (1979).
31. Bremer, N. J., and Dria, D. E., U.S. Patent 4,244,879 (1981).
32. Milberger, E. C., Bremer, N. J., and Dria, D. E., U.S. Patent 4,333,853 (1982).
33. Hutchins, N., and Higgins, D., U.S. Patent 4,209,423 (1980).
34. Ladwig, G., *Z. Chem.* **8,** 307 (1968).
35. Schroeder, L. W., Jordan, T. H., and Browen, W. E., *Spectrochim. Acta* **37**(A), 21 (1981).
36. Marchou, B., and Novak, A., *J. Chem. Phys.* **78,** 2105 (1983).
37. Bukovec, P., Milicev, S., Demson, A., and Golic, L., *J. Chem. Soc. Dalton,* 1802 (1981).
38. Labonnette, D., and Taravel, B., *J. Chem. Res.,* 34 (1984).
39. Lutz, H. D., Pobitschka, W., Frischemeier, B., and Becker, R.-A., *Appl. Catal.* **32,** 541 (1978).
40. Mereiter, K., Preiginger, A., Zellner, A., Mikende, W., and Steidl, H., *J. Chem. Soc. Dalton,* 1275 (1984).
41. Wilson, E. B., *Phys. Rev.* **45,** 706 (1934).
42. Ladwig, G., *Z. Anorg. Allg. Chem.,* **338,** 266 (1965).
43. Corbridge, D. E., and Lowe, E. J., *J. Chem. Soc.,* 4553 (1954).
44. Hezel, A., and Ross, S. A., *Spectrochim. Acta Part A* **24,** 131 (1968).
45. Cheng, S., Peng, G. Z., and Clearfield, A., *Ind. Eng. Chem. Prod. Res. Dev.* **23,** 219 (1984).
46. Dines, M. B., and Di Giacomo, P. M., *Inorg. Chem.* **20,** 92 (1981).
47. Johnson, J. W., Jacobson, A. J., Brody, J. F., and Lewandowski, J. T., *Inorg. Chem.* **23,** 3842 (1984).